PAMM

WILEY-VCH

SPECIAL ISSUE 94th Annual Meeting of the International Association of Applied Mathematics and Mechanics (GAMM)

PAMM Proceedings in Applied Mathematics and Mechanics

RESEARCH ARTICLE OPEN ACCESS

Mapping Shear Transformation Zones in Silica Network Glass

Somar Shekh Alshabab | Zhao Wu | Bernd Markert | Franz Bamer

Institute of General Mechanics, RWTH Aachen University, Aachen, Germany

Correspondence: Somar Shekh Alshabab (shekh.alshabab@iam.rwth-aachen.de)

Received: 31 May 2024 | **Revised:** 8 November 2024 | **Accepted:** 2 December 2024

ABSTRACT

Understanding nanoscale behavior in glasses is challenging due to their inherent long-range disorder and the absence of clearly defined defect regions. However, shear transformation zone theory suggests that certain "soft spots," which are prone to plastic rearrangements, can be identified even in stress-free configurations. Various predictive methods, such as energy approximations and local structural indicators, have been proposed with varying success. The local yield stress (LYS) method, however, has demonstrated strong potential by identifying these soft spots based on local mechanical properties. In this study, we use the LYS method to analyze the distribution of soft spots in 2D silica network glass, where the local critical stresses are probed using mechanical simulations. Samples with different heterogeneities are generated through a Monte Carlo bond-switching algorithm and subjected to shear via an athermal quasistatic (AQS) deformation protocol. Our results reveal a high correlation between regions with low critical stresses and the locations of rearrangement events, especially for events that happen early in the shear simulations, though this correlation decreases as the system approaches failure. These findings highlight the method's effectiveness in predicting plastic activity in structural glasses, and confirming that soft spots can be identified from the initial configuration. Additionally, we optimized the probing length scale for different levels of heterogeneity and analyzed the resulting statistical distributions of the local critical stresses, which are essential for accurate macroscopic modeling of silica glass.

1 | Introduction

Our understanding of the mechanisms behind the mechanical deformation of glasses has significantly advanced since Argon proposed that local clusters of atoms undergo shear transformations according to an Eshelby-like field [1]. In 1998, Falk et al. introduced a comprehensive theory on the dynamics of shear transformation zones (STZs) [2]. Since then, substantial efforts have been dedicated to predicting and studying these zones. Two main approaches have emerged for predicting STZs. The first approach involves approximations of the potential energy landscape (PEL). Harmonic approximations [3] have had limited success since it was shown that STZ involves the hybridization of localized vibrational mode with phonons [4]. On the other hand, anharmonic approximations have shown better predictive capability of STZs, offering a more accurate picture of deformation in glasses [5].

The second approach focuses on local structural indicators within the system. Key indicators include among others, the local elastic moduli [6], local yield stress (LYS) [7], and machine learning techniques [8]. Among these methods, LYS has proven to be highly accurate, effectively predicting the location of shear transformation zones by analyzing the local stress-free configuration. This high accuracy of the LYS method strongly supports that STZs are detectable in the stress-free configuration.

However, despite these advances, questions about the universality of the LYS method remain. While it has been successfully applied to binary glasses, it has yet to be tested on silicate glasses,

which have different structural and mechanical properties, where bond-breaking events become dominant due to covalent bonds [9, 10]. Further research is needed to explore the applicability of the LYS method to a broader range of glassy materials.

In this paper, we investigate the plasticity and fracture of 2D silica glass using molecular mechanics. Following the LYS method, we probe the local critical stresses to predict STZs in samples exhibiting different degrees of heterogeneity. These heterogeneities were introduced using a Monte Carlo bond-switching algorithm and subjected to true shear in athermal quasistatic (AQS) conditions. Our results demonstrate that the LYS method is able to predict the locations of elementary rearrangement events during plastic deformation. This supports the validity of the STZ concept as a general deformation mechanism in network glasses.

1.1 | Sample Generation

Glassy systems are characterized by a lack of long-range order, exhibiting only short- and mid-range order [11]. However, it has been shown in experimental images [12] that 2D silica glass follows the continuous random network theory [13]. The theory has the restriction that all atoms have to be fully coordinated, i.e., each silica atom is surrounded by three oxygen atoms. Achieving this structure is unfeasible using traditional melting-quenching techniques, so we employ a Monte Carlo bond-switching algorithm to generate the disorder [14].

Initially, we created a 2D crystalline silica network containing only six-fold rings. A Monte Carlo simulation is then performed, where bond switches are attempted between randomly selected pairs of silicon atoms. These bond switches, which are carried in the dual lattice space, alter the ring size distribution and introduce disorder into the system. Bond switches that result in over- or under-coordination are immediately rejected, and another switch is attempted. The acceptance probability of a switch is determined using the Metropolis–Hastings criterion. To model disorder, we approximate the ring size distribution with a logarithmic distribution function [15]:

$$P(x_n, \mu^{(m)}, \sigma^{(m)}) = \frac{1}{\sigma x_n \sqrt{2\pi}} \exp \frac{(\log x_n - \mu^{(m)})^2}{2\sigma^{(m)2}}, \tag{1}$$

where x_n is the continuous counterpart to the ring size integer values, and $\mu^{(m)}$ and $\sigma^{(m)}$ are the mean and standard deviation, respectively. The parameter $\mu^{(m)}$ is taken from experimental values, while $\sigma^{(m)}$ is varied to control the disorder in the system. However, taking into consideration only global ring statistics in the bond-switching algorithm may lead to unphysical local clusters of atoms. Therefore, we incorporate ring neighborhood statistics using the empirical Aboav–Weaire law [16–18]:

$$m_a = \mu_n(1 - \alpha_n) + \frac{\mu_n^2 \alpha_n + \sigma_n^2}{n}, \tag{2}$$

where m_n is the mean ring size naturally found around rings of size n. Here, μ_n and σ_n are the mean and standard deviation of ring statistics, and α_n, which typically takes values around 0.3, indicates that smaller rings are more likely to be surrounded by larger ones. An objective function is then constructed based on the parameters σ_m from Equation (1) and α_n from Equation (2), which is used to adapt the Metropolis–Hastings condition.

Furthermore, after each bond, switching the potential energy of the system is minimized to ensure that the configuration of the system is in static equilibrium. The minimization of the energy is carried out using the Yukawa potential [19–21]. This potential is commonly used to describe silica network glass [21–24]. The potential takes the following form:

$$\tilde{U}_2(r_{ij}) = \left(\frac{a_{ij}}{r_{ij}}\right)^{12} + \frac{q_{ij}}{r_{ij}} \exp(-\kappa r_{ij}), \tag{3}$$

where r_{ij} is the inter-atomic distance, q_{ij} refers to charge, a_{ij} denotes the repulsive strength and κ is the screening parameter. The cut-off radius of the potential was set to 10 Å. It is worth mentioning that this potential reproduces the experimental short-range order and ring statistics in 2D silica glass well [22].

In this paper, we used the aforementioned procedure to simulate 2D silica network glasses with varying variances in the distribution of ring structures, which serve as a measure of the system's heterogeneity. Specifically, we studied five different levels of heterogeneity: 0.6, 0.8, 1.0, 1.2, and 1.4. For each level, 50 samples were generated, each containing 9600 atoms, comprising 5760 oxygen atoms and 3840 silica atoms.

1.2 | Mechanical Simulation

The mechanical simulations are done using the AQS protocol [25] with periodic boundary conditions (PBCs). The AQS algorithm consists of two primary actions, which are repeated throughout the simulation. At each deformation step, an affine deformation field is applied, followed by minimization of the potential energy, resulting in the non-affine movement of atoms. This process ensures that the system remains in equilibrium throughout the simulation. This method is widely employed in molecular dynamics due to its ability to approximate low strain rates ($\dot{\varepsilon} \to 0$), which are not achievable using conventional MD simulation techniques. Additionally, it facilitates easier identification of the material's mechanical responses by suppressing thermal effects.

Each sample is subjected to an external true shear strain field through 400 deformation steps, each with a displacement of $\Delta x = 0.1$ Å along the x_1-axis. The stress–strain curves of the systems exhibit linear branches interrupted by sudden drops, indicating the jerky motion of the system. The linear branches represent the elastic response of the system, while the sudden drops correspond to rearrangement events of the atoms, where the minimum in the PEL flattens out, causing the system to transition to a new configuration. These events represent STZs [2]. The step size was carefully chosen to ensure that no elementary event was missed during the simulation.

The stress–strain curves are analyzed for the stress drops. At each stress drop, the displacement fields before and after the event are extracted. Consequently, the non-affine displacement field for

each event is computed by subtracting the affine displacements from the total displacement field. Furthermore, the location of the atom undergoing the largest non-affine displacement is considered the center of the rearrangement event.

1.3 | Local Critical Stresses

Patinet et al. [7] demonstrated that the LYS method is a powerful tool for predicting plastic activity in amorphous solids. This method is based on the concept that different local spots in the system have varying stress thresholds, which, when exceeded, cause the system to fall out of equilibrium. This concept is widely used in macroscopic descriptions of amorphous solids [26], making this method particularly useful for upscaling approaches.

At each grid point, a circular region with a radius $r_{tot} = r_{free} + r_{cut}$ is defined, which is subjected to an AQS shear deformation protocol, where r_{cut} is the cutoff radius potential used in the simulation. The atoms in the region between r_{free} and r_{tot} are constrained to move purely affinely, and therefore, constitute a boundary region for the atoms in the region within r_{free}, which are left to move freely. All the atoms outside r_{tot} are removed to save computational time.

The same deformation protocol used for the entire system is applied to the individual spots. Specifically, an AQS true shear protocol is followed with deformation steps of $\Delta x = 0.1$ Å. During energy minimization, only the atoms within r_{free} are relaxed. The shear simulation continues until a decrease in the P_{11} component of the virial stress tensor is detected. At this point, the stress is recorded, and the simulation is stopped. The difference between the initial stress and the stress just before the drop is taken to be the critical stress of the region.

Due to the anisotropic nature of the material, the local critical stress is measured in multiple directions. Each region is rotated, and the shear simulation is repeated in the x_1-direction, with rotations from $\alpha = 0°$ to $\alpha = 170°$ in increments of $\Delta\alpha = 10°$. This process provides a direction-dependent local threshold $P^c_{11}(\alpha)$ for each spot, which is crucial for understanding the anisotropy of the system. Notably, at higher heterogeneity and larger sizes, the overall system anisotropy decreases, but the defined local spots exhibit strong anisotropy. Our shear simulation of the complete system is conducted along the x_1-axis. Therefore, for each spot, the local critical stress as a function of α is computed by projecting the stress onto the x_1-axis, i.e., at $\alpha_l = 0°$. To obtain a scalar quantity that aids in predicting active plastic zones, we take the local critical stress to be the minimum of all the values:

$$\Delta P_{11}^{crit} = \min_{\alpha} \frac{\Delta P^{c}{}_{11}(\alpha)}{cos[2(\alpha - \alpha_l)]}. \quad (4)$$

An illustrative drawing of the method is presented in Figure 1. To assess whether the local critical stresses provide valid predictions for plastic activity, we correlate the generated data with rearrangement events from the shear simulations. We begin by computing the cumulative distribution function (CDF) of all the grid points in one sample. Next, we map the locations of the rearrangement events back onto our created grid and extract the corresponding CDF values. We then compute a prediction goodness measure C_Ψ, defined for a certain local threshold as follows [7]:

$$C_\Psi = 1 - 2\bar{\text{CDF}}(\Psi_{i_{max}}). \quad (5)$$

Here, Ψ is the local threshold measure, which in our case is ΔP_{11}^{crit}. $\bar{\text{CDF}}$ is the cumulative distribution function averaged over all the samples of a certain heterogeneity. If the rearrangement events occur near grid points with low critical stress and therefore a low value of the CDF, the goodness values approach a value of one, which means perfect prediction. Consequently, the values of C_Ψ range from 1 for perfect correlation to -1 for perfect anticorrelation.

2 | Results

2.1 | LYS statistics

To study our systems, we need to define r_{free}, which remains a free parameter. Therefore, we conduct a parametric study by varying r_{free} from 6.0 to 14.0 Å in increments of 0.5 Å. Using each radius, we analyze the initial configuration of each system (the configuration at the beginning of the shear simulation) using the previously described method. An example of the local critical stress map for two systems with different heterogeneities, produced using different scanning radii, is shown in Figure 2.

First, we compute the global probability distribution functions (PDFs) of all the spots for each heterogeneity using different free radii. The results are plotted in Figure 3. In Figure 3a, where $r_{free} = 6.0$ Å, the distribution is symmetric and sharply peaks around 0.5. However, for lower heterogeneities, the distribution is slightly broader with a peak shifted toward higher values. At higher radii, $r_{free} = 12.0, 13.0$, and 14.0 Å, as shown in Figure 3e, f, and g, respectively, the distribution becomes wider, the skewness increases, and the peak shifts toward higher values.

Figure 3b–d show that lower heterogeneities transition to a skewed distribution at lower radii. As the free radius increases, the PDFs of different heterogeneities initially diverge but then converge again at higher radii, displaying similar distributions. This widening and skewing of the PDFs can be partially explained by the "spill-over" effect of regions with low critical stress. As the free radius increases, unstable regions are more likely to be included in the spots of neighboring regions. This phenomenon is illustrated in Figure 2.

2.2 | Prediction Goodness

First, we only analyze the first event of the shear simulation for each sample to determine which radius provides the best prediction goodness. The results are plotted in Figure 4a. It is evident that smaller radii do not yield good predictions for all heterogeneities. However, as the free radius increases, the prediction goodness significantly improves and converges to values close to one, indicating a strong correlation between the first rearrangement events and regions with low critical stress. Notably, the convergence of prediction goodness occurs

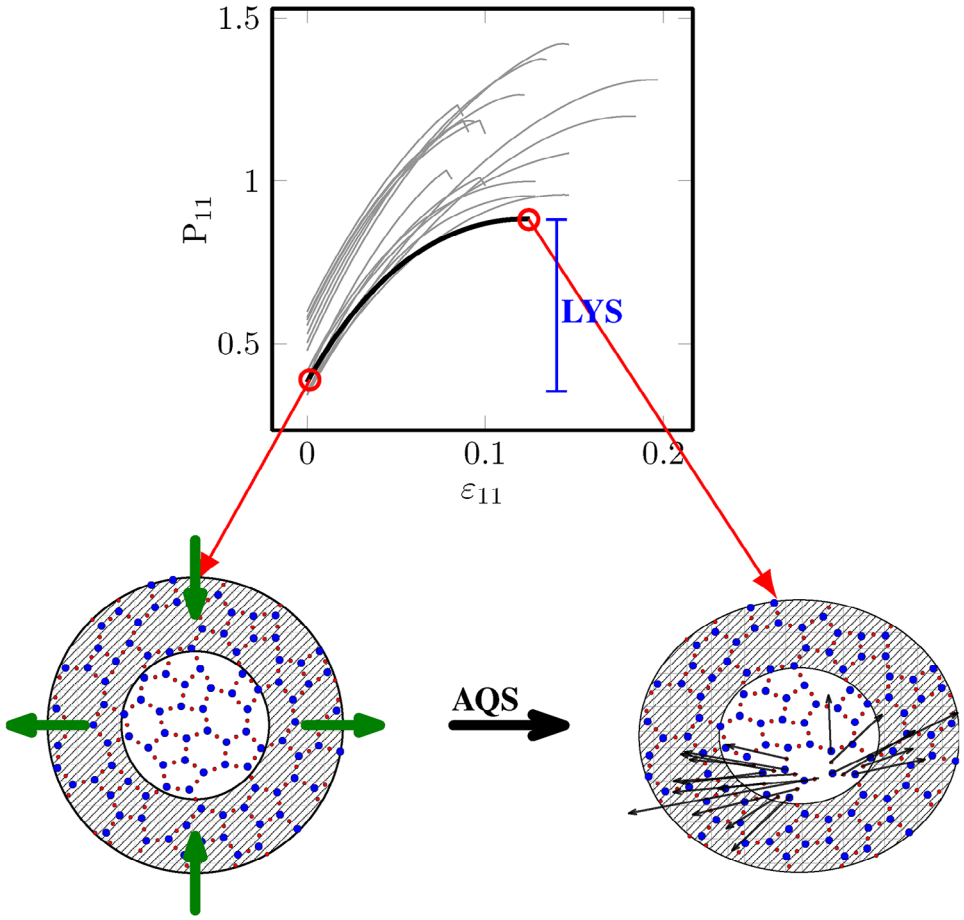

FIGURE 1 | An illustration of the local critical stress method. Atoms within the inner circle are free to move during the simulation, while atoms in the shaded area (the outer ring) are frozen, creating rigid boundary conditions. All other atoms in the system are removed, and the system is subjected to shear deformations using AQS protocol until a stress drop occurs. This stress drop could happen when a bond breaks, as shown above, or at yielding, where the stress plateaus. The black arrows in the second figure indicate the non-affine displacement field at the stress drop. The local critical stress for a specific angle is then taken as the difference between the maximum stress and the initial stress. This process is repeated for different rotation angles α of the spot. In the upper plot, the P_{11} component from the virial stress tensor $\mathbf{P}$ is plotted for a single spot at rotation angles ranging from $\alpha = 0$ to $\alpha = 170$ Å in increments of $\Delta\alpha = 10$ Å. The local critical stress is measured from the black curve, as it satisfies the criteria in Equation (4). AQS, athermal quasistatic.

at higher radii for higher heterogeneities. Additionally, the first events in systems with higher heterogeneities exhibit lower prediction goodness.

The first plastic event typically occurs within the elastic regime of the material. However, our interest extends to studying plastic activity during yielding and fracture. Therefore, we compute the prediction goodness for the first 15 events of each heterogeneity. The results are shown in Figure 4b. The average prediction goodness for higher radii remains high, above 0.8, for most heterogeneities ($\sigma = 0.8$ to $\sigma = 1.4$), and slightly lower for heterogeneities $\sigma = 0.6$ and $\sigma = 0.7$. Interestingly, we observe the opposite trend compared to the first events: later events are harder to predict in lower heterogeneities. This can be attributed to the more brittle nature of the material with lower disorder. Consequently, the system enters the fracture regime earlier in the simulation, where avalanche events of crack propagation become more common [27]. Crack propagation events are expected to show a lower correlation with regions with low critical stresses since they result from stress concentration around bonds broken in earlier events. Furthermore, the method used to measure the goodness does not account for events composed of multiple subevents.

Based on the results presented in Figure 4, our objective is to determine the optimal free radius necessary for predicting plastic events within various heterogeneities. The prediction goodness in Figure 4 converges to values close to its maximum and stabilizes above a certain radius, resulting in multiple consecutive radii yielding similar values within an error margin. Therefore, we consider the optimal radius to be the smallest radius that provides the maximum prediction goodness within a 1% error margin.

This optimal radius offers insights into the minimum degrees of freedom required within a local spot for the local mechanical probing to accurately predict consecutive elementary events. The results are presented in Figure 5a. For the first event, the optimized free radius correlates with the level of disorder, with larger radii providing better predictions for systems with higher heterogeneities. Intriguingly, this trend reverses when

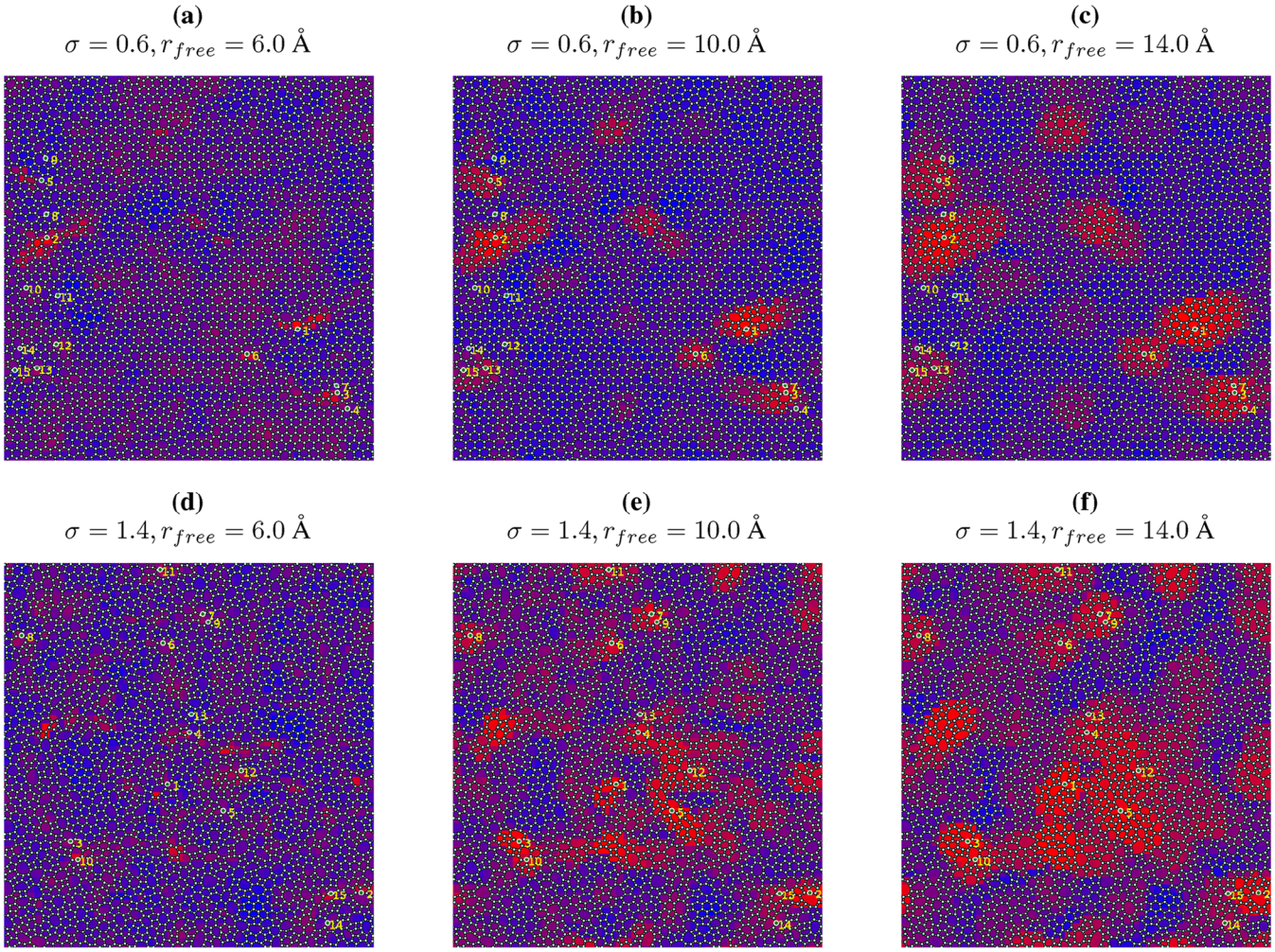

FIGURE 2 | Map of the local critical stresses for two different heterogeneities and for different r_{free}. The blue color represent regions with high critical stresses, while the red spots represent regions with low values, which indicate regions that are susceptible to rearrangement events. The markers represent the rearrangement events extracted from the true shear simulation, while the numbers indicate the order of these events.

considering the first 15 events: larger radii yield better predictions for systems with lower heterogeneity.

Additionally, both trends converge for systems with heterogeneity $\sigma = 1.3$ and $\sigma = 1.4$, indicating that the optimized radius is effective for predicting either the first or the first 15 events.

In Figure 5b, the prediction goodness for the first 40 events is plotted using the computed optimized r_{free} for heterogeneities $\sigma = 0.6$, 0.8, 1.0, 1.2, and 1.4. For the lower heterogeneities, the prediction goodness drops sharply, reaching values close to zero after around 15 events, indicating that the prediction at this point is only slightly better than random. However, as the heterogeneity increases, the prediction goodness for later events also increases. For the higher heterogeneities, the prediction goodness decreases linearly until the 40th event.

Considering that this method only scans the initial configuration and does not account for the sequence of events, this suggests that plastic activity in highly disordered systems remains correlated with the initial configuration for a longer time.

It is worth noting that we chose to stop at the 15th event for the optimization of the free radius because predictions become close to random for lower heterogeneities beyond this point. However, when using the first 40 events instead of the first 15, we observe very similar trends.

Our analysis of two-dimensional silica glass using the described method aligns with findings by Patinet et al. for two-dimensional Lennard-Jones (LJ) glass, demonstrating a high correlation between regions with low critical stresses and the locations of rearrangement events. These results confirm the robustness of the method for predicting different types of elementary events, including bond-breaking, which are characteristic of silica's covalent network. Intriguingly, the bond-breaking phenomenon is also observed in local mechanical simulations of the spots. Furthermore, additional differences appear in the statistical distributions of the thresholds. Our data show that at small probing radii, the threshold distributions are symmetric and sharply peaked. As the radius increases, these distributions broaden and develop a left-skew. In contrast, two- and three-dimensional binary glasses display right-skewed distributions [28, 29].

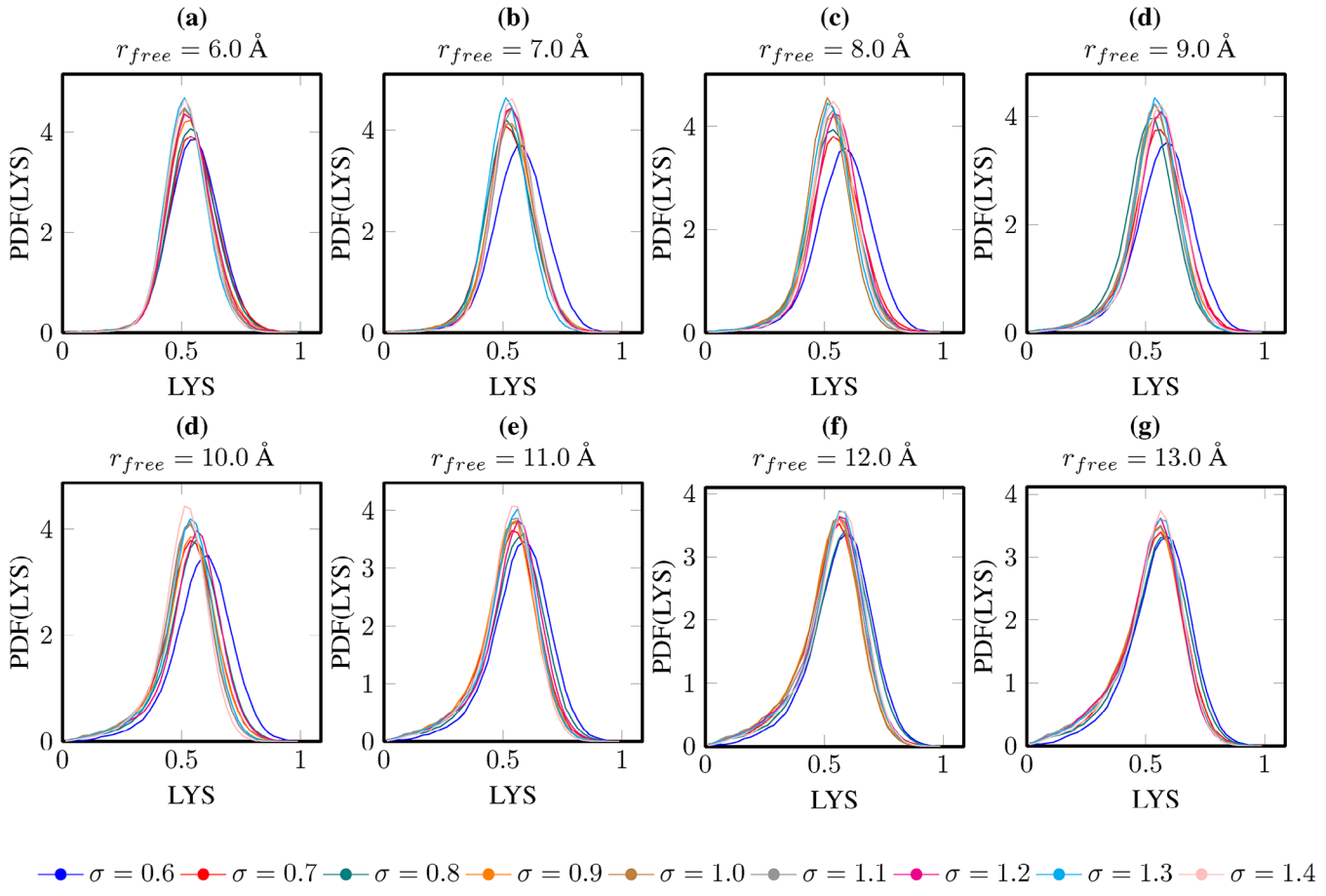

FIGURE 3 | Probability density function of the local critical stresses of each heterogeneity and for free radii from $r_{free} = 6.0$ Å (a) until $r_{free} = 13.0$ (g) Å.

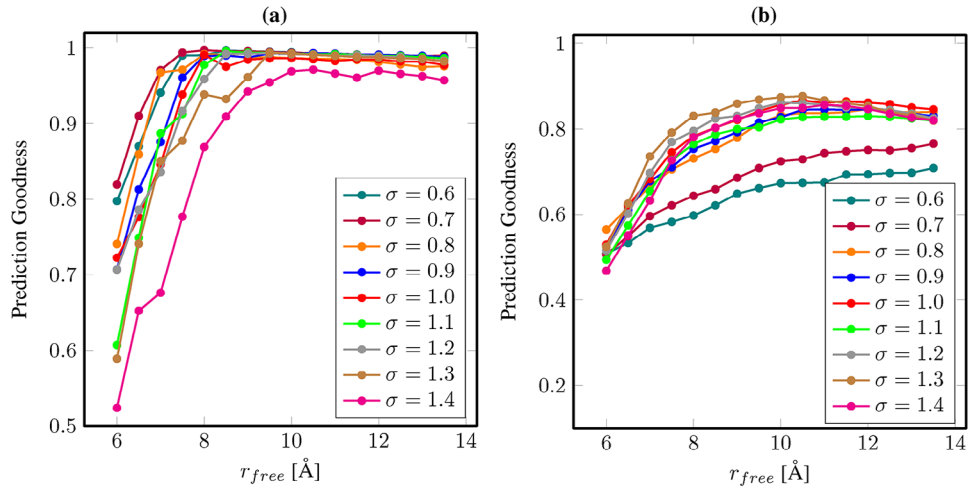

FIGURE 4 | Prediction goodness of different free radii r_{free} of the elementary events for the systems with different heterogeneities, (a) prediction goodness of the first event; (b) average prediction goodness for the first 15 events.

3 | Conclusion

Following LYS method, we used local mechanical probing to compute the local critical stresses and predict plastic rearrangement events in 2D silica network glass. We demonstrated that the method has remarkable predictive power for plastic activity in our systems. The results indicate a strong correlation between the regions identified by the method and the locations of local rearrangement events akin to STZs. This confirms that these spots are predictable from the initial configuration.

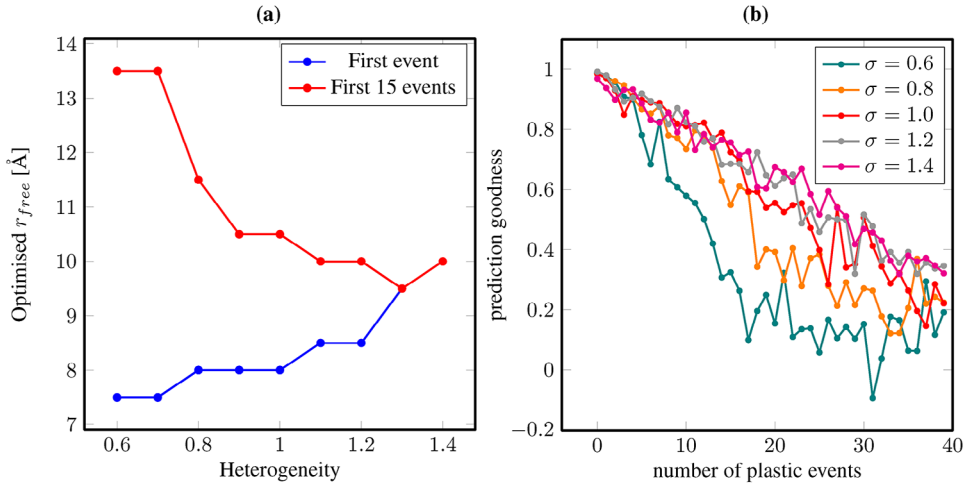

FIGURE 5 | (a) The optimized free radius used for the computation of the local critical stresses that are used for the prediction of rearrangement events for different heterogeneities. (b) The prediction goodness plotted against the number of plastic events for heterogeneities $\sigma = 0.6$, 0.8, 1.0, 1.2, and 1.4, using the optimized radius for each. For better visibility of the results, other heterogeneities were omitted.

By scanning our systems with various free radii, we found that larger radii yield different statistical distributions of the local critical stresses, producing wider and more skewed distributions. The shape of these distributions is valuable for macroscopic modeling of disordered materials. Furthermore, our results show that the optimal radius for predicting the first rearrangement event correlates with the level of disorder in the system. Surprisingly, for predicting a larger number of events, this trend reverses, and a relatively smaller radius provides the best prediction.

Finally, while our study highlights the high correlation between regions with low local critical stresses and the locations of plastic events, questions remain about whether this is sufficient for modeling plasticity in disordered solids. Additionally, avalanche events play a central role in fracture of silica glass [27] and extending the method to consider them seems like the logical next step. This could be done by careful analysis of the interaction of the STZs similarly to the interactions of defects [30, 31]. However, this is beyond the scope of this study and is left for future investigations.

Acknowledgments

This research was funded by the Deutsche Forschungsgemeinschaft (DFG, German Research Foundation) Project No. 523939420). Furthermore, the computations were performed with computing resources granted by RWTH Aachen University under Project No. p0020324.

Open access funding enabled and organized by Projekt DEAL.

References

1. A. S. Argon, "Plastic Deformation in Metallic Glasses," *Acta Metallurgica* 27 (1979): 47.

2. M. L. Falk and J. S. Langer, "Dynamics of Viscoplastic Deformation in Amorphous Solids," *Physical Review E* 57 (1998): 7192.

3. G. Kapteijns, D. Richard, and E. Lerner, "Nonlinear Quasilocalized Excitations in Glasses: True Representatives of Soft Spots," *Physical Review E* 101 (2020): 032130.

4. L. Gartner and E. Lerner, "Nonlinear Modes Disentangle Glassy and Goldstone Modes in Structural Glasses," *SciPost Physics* 1 (2016): 016.

5. D. Richard, G. Kapteijns, J. A. Giannini, M. L. Manning, and E. Lerner, "Simple and Broadly Applicable Definition of Shear Transformation Zones," *Physical Review Letters* 126 (2021): 015501.

6. M. Tsamados, A. Tanguy, C. Goldenberg, and J. L. Barrat, "Local Elasticity Map and Plasticity in a Model Lennard-Jones Glass," *Physical Review E* 80 (2009): 026112.

7. S. Patinet, D. Vandembroucq, and M. L. Falk, "Connecting Local Yield Stresses with Plastic Activity in Amorphous Solids," *Physical Review Letters* 117 (2016): 045501.

8. E. D. Cubuk, S. S. Schoenholz, J. M. Rieser, et al., "Identifying Structural Flow Defects in Disordered Solids Using Machine-Learning Methods," *Physical Review Letters* 114 (2015): 108001.

9. F. Bamer, S. S. Alshabab, A. Paul, F. Ebrahem, B. Markert, and B. Stamm, "Data-Driven Classification of Elementary Rearrangement Events in Silica Glass," *Scripta Materialia* 205 (2021): 114179.

10. F. Ebrahem, F. Bamer, and B. Markert, "Origin of Reversible and Irreversible Atomic-Scale Rearrangements in a Model Two-Dimensional Network Glass," *Physical Review E* 102 (2020): 033006.

11. F. Bamer, F. Ebrahem, B. Markert, et al., "Molecular Mechanics of Disordered Solids," *Archives of Computational Methods in Engineering* 30 (2023): 2105–2180.

12. P. Y. Huang, S. Kurasch, J. S. Alden, et al., "Imaging Atomic Rearrangements in Two-Dimensional Silica Glass: Watching Silica's Dance," *Science* 342 (2013): 224.

13. W. H. Zachariasen, "The Atomic Arrangement in Glass," *Journal of the American Chemical Society* 54 (1932): 3841.

14. F. Ebrahem, F. Bamer, and B. Markert, "Vitreous 2D Silica Under Tension: From Brittle to Ductile Behaviour," *Materials Science and Engineering: A* 780 (2020): 139189.

15. C. Büchner, L. Liu, S. Stuckenholz, et al., "Building Block Analysis of 2D Amorphous Networks Reveals Medium Range Correlation," *Journal of Non-Crystalline Solids* 435 (2016): 40.

16. D. Aboav, "The Arrangement of Grains in a Polycrystal," *Metallography* 3 (1970): 383.

17. D. Aboav, "The Arrangement of Cells in a Net," *Metallography* 13 (1980): 43.

18. D. Weaire, "Some Remarks on the Arrangement of Grains in a Polycrystal," *Metallography* 7 (1974): 157.

19. G. A. Méndez-Maldonado, M. González-Melchor, and J. Alejandre, "Liquid-Vapor Phase Biagram and Cluster Formation of Two-Dimensional Ionic Fluids," *Journal of Chemical Physics* 137 (2012): 054711.

20. G. A. Méndez-Maldonado, M. González-Melchor, and J. Alejandre, "Phase Equilibria and Interfacial Properties of Two-Dimensional Yukawa Fluids," *Condensed Matter Physics* 15 (2012): 23002.

21. P. K. Roy, M. Heyde, and A. Heuer, "Modelling the Atomic Arrangement of Amorphous 2D Silica: A Network Analysis," *Physical Chemistry Chemical Physics* 20 (2018): 14725.

22. P. Roy and A. Heuer, "Relating Local Structures, Energies, and Occurrence Probabilities in a Two-Dimensional Silica Network," *Journal of Physics: Condensed Matter* 31 (2019): 225703.

23. F. Bamer, F. Ebrahem, and B. Markert, "From DFT to Machine Learning: Recent Approaches to Materials Science—A Review," *Journal of Physics: Materials* 163 (2019): 301–307.

24. F. Bamer, F. Ebrahem, and B. Markert, "Elementary Plastic Events in a Zachariasen Glass Under Shear and Pressure," *Materialia* 9 (2020): 100556.

25. C. E. Maloney and A. Lemaître, "Amorphous Systems in Athermal, Quasistatic Shear," *Physical Review E* 74 (2006): 016118.

26. D. Vandembroucq and S. Roux, "Mechanical Noise Dependent Aging and Shear Banding Behavior of a Mesoscopic Model of Amorphous Plasticity," *Physical Review B* 84 (2011): 134210.

27. S. S. Alshabab, B. Markert, and F. Bamer, "Criticality in the Fracture of Silica Glass: Insights From Molecular Mechanics," *Physical Review E* 109 (2024): 034110.

28. A. Barbot, M. Lerbinger, A. Hernandez-Garcia, et al., "Local Yield Stress Statistics in Model Amorphous Solids," *Physical Review E* 97 (2018): 033001.

29. D. Ruan, S. Patinet, and M. L. Falk, "Predicting Plastic Events and Quantifying the Local Yield Surface in 3D Model Glasses," *Journal of the Mechanics and Physics of Solids* 158 (2022): 104671.

30. F. Ebrahem, F. Bamer, and B. Markert, "StoneWales Defect Interaction in Quasistatically Deformed 2D Silica," *Journal of Materials Science* 55 (2020): 3470–3483.

31. T. Focks, F. Bamer, B. Markert, Z. Wu, and B. Stamm, "Displacement Field Splitting of Defective Hexagonal Lattices," *Physical Review B* 106 (2022): 014105.